



Radiation-induced lung injury patterns and the misdiagnosis after SBRT of lung cancer

Xueru Zhu¹, Xiaoyang Li¹, Hengle Gu, Wen Yu*, Xiaolong Fu*

Department of Radiation Oncology, Shanghai Chest Hospital, Shanghai Jiao Tong University, Shanghai, 200030, China

ARTICLE INFO

Keywords:

Lung cancer
Stereotactic body radiotherapy
Radiation-induced lung injury
Predictive model

ABSTRACT

Purpose: To analyze radiation-induced lung injury (RIL) after stereotactic body radiotherapy (SBRT) of lung cancer and the subsequent clinical problems.

Methods: 106 lung cancer patients treated with SBRT were included, their computed tomography (CT) scans were reviewed. Late injury pattern was classified by Koenig's, radiologist' diagnosis reports for RIL was reviewed. Logistic regression was used to analyze the predictive model of injury pattern, which was also validated by ROC curve.

Results: Radiographic late injury within at least 6 months after SBRT was concluded. The majority of late RIL was mass-like pattern, not the modified conventional pattern. 36.8% patients showed acute injury, which trend to occur late lung injury earlier than patients who were not found acute injury ($p = 0.0185$). 24.5% RIL cases were misdiagnosed to tumor progression by radiologists. Most misdiagnosis occurred among mass-like pattern. Per fraction dose ($p < 0.0001$), prescription isodose line ($p = 0.027$) and age ($p = 0.089$) trend to associate with the occurrence of mass-like injury pattern. Nomogram was established based on these parameters, ROC curve showed that area under the ROC curve (AUC) of the nomogram was 0.767 (95% CI = 0.677-0.857), which was better than any factors along.

Conclusion: SBRT for lung cancer patients was safe, the majority of late RIL was mass-like pattern. This injury was difficult to be distinguished from tumor progression, which led to misdiagnosis of 24.5% patients receiving SBRT. A nomogram based on age, per fraction dose and the prescription isodose line may assist the diagnosis in clinical practice.

1. Introduction

Stereotactic body radiation therapy (SBRT), also known as stereotactic ablative radiotherapy, is currently the standard modality for early-stage inoperable non-small cell lung cancer (NSCLC) [1]. It utilizes several beams from different angles to cross-fire with high dose precisely to tumors. Previous study showed that average 3-year local control (LC) rate was 86.7% and 3-year overall survival (OS) rate was 59.6% [2]. In addition, the LC rate is also increasing in recent years due to recent technological development [3]. Due to the high efficacy, SBRT has also been proposed to play a role in younger and healthier patients and oligo-metastasis NSCLC.

However, the high dose per fraction and biological effective dose of SBRT results in significantly different radiation-induced lung injury patterns compared with that of conventional radiotherapy [4]. Therefore, it's crucial to analyze radiological changes after SBRT and further

distinguish radiation-induced injury from tumor recurrence.

From the radiobiological perspective, high dose of per fraction may exert more effects on late injury than early injury [5]. Here, we mainly described three topics: The late injury patterns of SBRT, the diagnostic descriptions of radiologists for late injury patterns and the potential predictive model of injury pattern.

2. Methods and materials

2.1. Patients

Between January 2015 and May 2018, 106 consecutive patients underwent SBRT for primary lung cancer and their follow-up CT images were reviewed at our institution. Inclusion criteria: (1) SBRT to primary lung cancer and (2) regular follow-up CT scans 6 months post-SBRT at the department of radiation oncology at the Shanghai Chest hospital.

* Corresponding authors.

E-mail addresses: yuzhiwen0827@163.com (W. Yu), xlful964@126.com (X. Fu).

¹ These authors contributed equally to this work.

Exclusion criteria: (1) lung metastases, (2) re-irradiation therapy, (3) No follow-up in our institution, (4) follow-up CT scans within 6 months post-SBRT. Demographic and tumor characteristics of patients were analyzed and all follow-up CT images were reviewed.

2.2. CT examination and treatment

CT examination of all patients were performed by using a 16-detector row scanner (Toshiba Aquilion, Japan) or 64-detector row scanner (Philip brilliance, Netherlands). Before performing dynamic CT, targeted thin-section helical CT scans (1.0 mm collimation, 0.4 s gantry rotation time, 120 kVp, 200 mA) were obtained from lung apices to the level of the middle pole of both kidney for tumor staging. Image data were reconstructed with a thickness of 2.0 mm using standard and lung algorithm, respectively. Iopamidol (370 mg I/ml, Bracco, Milan, Italy) was administered at a rate of 4 ml/s, 420 mg/kg with a power injector (MCT Plus, Medrad, Pittsburgh, Pa), followed by a 20 ml of saline solution at the same rate.

A vacuum cushion (Human positioning cushion, C 100*80, Shanghai Lanya Electronic Technology Development Co., Ltd.) was used to immobilize patient. Patients lay on the CT simulator bed with hands crossing and placing on the forehead and received CT scan under free breath. Because our institution was not equipped with 4D-CT which can record breathing cycle to define the internal gross target volume, we implemented CT scan for three times to ascertain the motion range of tumors. The entire thorax was scanned for only once with 3 mm thickness and the tumor lesion was scanned for two times with 1 mm thickness. All the three sets of images were registered and fused in the treatment planning system (Pinnacle). Gross tumor volume (GTV) was delineated on each image set and the maximization of the three GTVs constituted the final internal tumor volume (ITV). ITV was expanded 5 mm into planning tumor volume (PTV). The tumor motion was also evaluated under X-ray simulator to confirm if the tumor ranged within ITV. Patients were treated according to the institutional SBRT protocol. Most patients received a dose of 50 Gy in 4 fractions or 5 fractions, and 60 Gy in 8 fractions. The treatment was implemented every other day. The Kilovoltage cone-beam CT (KVCBCT) scan were utilized before treatment to reduce setup errors. 6 MV X-ray was used and usually 10–15 beams were arranged for treatment.

2.3. Evaluation

Patients were followed up with thorax CT scans at 1, 3, 6 months post-SBRT and thereafter every half year. Considering radiobiological theory that the very high doses of per fraction may have a deeper effect for late injury than early injury, here we mainly evaluated and classified late lung injury. One radiologist and one radiation oncologist reviewed all of the CT scans. According to Koenig [6], we classified the CT appearance of radiation fibrosis (at least 6 months post-SBRT) into four patterns: (1) non-injury, no visible lung injury; (2) modified conventional, consolidation, volume loss and bronchiectasis which is similar to but less extensive than conventional radiation fibrosis; (3) mass like, focal consolidation limited around the tumor; (4) scar like, linear opacity in the region of tumor and associated with volume loss. For acute radiation pneumonitis (less than 6 months after SBRT), we just evaluated whether lung injury exist. We also assessed the late injury of radiation fibrosis by Common Terminology Criteria for Adverse event 5.0 (CTCAE 5.0) [7]. Grade 1, radioactive fibrosis less than 25% of lung volume with hypoxia; Grade 2, there is evidence of pulmonary hypertension, radiation pulmonary fibrosis is 25%–50% lung volume with hypoxia; Grade 3, severe hypoxia, evidence of right heart failure, radioactive pulmonary fibrosis is 50%–75% lung volume; Grade 4, life-threatening, such as hemodynamic or pulmonary complications, assisted ventilatory intubation, radiation-induced pulmonary fibrosis greater than 75% lung volume with severe cell-like changes; Grade 5, died of radioactive fibrosis.

In addition, we reviewed and concluded the diagnostic description of radiologists and classified the diagnosis into three main descriptions: tumor progression, which clearly indicated that the mass was tumor and progressed than previous; objective description, just described the visible imaging changes, without mentioning tumor progression or treating injury; radiation injury, clearly pointed out the change was injury after radiotherapy.

2.4. Statistical analysis

Univariate and multivariate analysis were conducted by logistic regression. The factors with $p < 0.05$ and in the equation of multivariate analysis were used to build the nomogram predictive model. Then, AUC of ROC curve was conducted to validate the nomogram.

Statistical analysis was performed using SPSS software, version 22.0 and R software, version 3.4.5. All tests were two-sided, $p < 0.05$ was defined as statistical significance.

3. Results

3.1. Patients' baseline

Patients' and tumors' characteristics are shown in Table 1. 106 patients with lung cancer receiving SBRT in our institution were included. The median age was 67 years old. 71 patients were male and 35 were female. All patients were diagnosed with primary lung cancers, among which 49 patients were T1-2N0M0 and Any T any N M1 for 57 patients. 87 lesions were located peripherally and other 19 lesions were located centrally. Due to limitation of current biopsy technique, only 75 (70.8%) patients were pathologically diagnosed with non-small cell lung cancer and the remaining patients were diagnosed by imaging: 8 (7.5%) patients by PET-CT and 23 (21.7%) patients by chest CT scan. All patients underwent diagnostic chest CT examination before treatment. In addition, generally, all patients have to take simulated location CT before making radiotherapy planning. Among all of these lesions, 8 were ground glass opacity (GGO). The median follow-up time was 1.14 years.

3.2. CT appearance of radiation injury

By comparing the CT scans before treatment and after SBRT, among the 106 patients, nobody had pulmonary fibrosis before SBRT. In 106 lesions, CT appearance of late radiation fibrosis were classified as follows: 13 were no injury (12.3%), 35 were modified conventional pattern (33.0%), 42 were mass-like pattern (39.6%), and 16 were scar-like pattern (15.1%) (Supplement Fig. 1). Mass-like and modified conventional patterns were the two most frequently seen radiation fibrosis (Fig. 1). 39 patients were observed with acute injury and 63 patients with no injury. 4 patients could not be evaluated due to pleural effusion. We found that all of the acute injury progressed to late injury, while 79.6% patients without acute injury still occurred late injury. Moreover, late lung injury occurred earlier among patient who were observed acute injury than patients who were not found acute injury ($p = 0.0185$) (Fig. 2). However, there was no difference of the first occurrence time of late lung injury among different injury pattern (Supplement Fig. 2). The median occurring time was 8 months and 4 months for late injury and early injury respectively. According to CTC 5.0, 93 (87.7%) patients occurred only grade 1 radiation fibrosis and 13 (12.3%) patients without radiation fibrosis. No grade 2–5 radiation fibrosis was observed. Retrospectively reviewing the diagnosis reports, we found that 26 (24.5%) late RIL cases were misdiagnosed with tumor progression. Most misdiagnosis occurred in mass-like pattern (46.2%) and conventional pattern (34.6%). Only 14 (13.2%) patients of RIL were diagnosed accurately with radiation injury, among which most patients were classified as modified conventional pattern (50%) and scar-like pattern (35.7%). In most diagnosis reports (66, 62.3%),

Table 1
Patient and tumor characteristics (n = 106).

Characteristic	Value (%)
Age, years	
≥ 70	47 (44.3)
< 70	59 (55.7)
Gender	
Male	71(67.0)
Female	35(33.0)
Tumor size (cm)	
≤ 3	88(83.0)
> 3	18(17.0)
Tumor Location	
Peripheral	87(82.1)
Central	19(17.9)
TNM stage	
T1-2N0M0	49(46.2)
Any T any N M1	57(53.8)
Diagnose basis	
Biopsy pathology	75(70.8)
PET-CT	8(7.5)
Chest CT	23(21.7)
Lesion appearance	
Consolidation nodule	98(92.5)
GGO	8(7.5)
Fractionation (Gy/Fractions)	
50/4	22(20.7)
50/5	50(47.2)
70/10	4(3.8)
60/8	19(17.9)
60/10	2(1.9)
50/10	4(3.8)
30/5	4(3.8)
49/7	1(0.9)
Acute injury	
Yes	39(31.0)
No	63(59.4)
Pulmonary Fibrosis Grade (CTC 5.0)	
0	13(12.3)
I	93(87.7)
Atelectasis	
Yes	13(12.3)
No	93(87.7)

GGO, Ground Glass Opacity.

radiologists described the visible radiological change without confirming tumor progression or treating injury (Fig. 3). In all of lesions, 13 (12.3%) patients were observed with atelectasis. By reviewing patients' radiotherapy plan and delineating the PBT, we found that some patients with atelectasis indeed received high dose of irradiation to PBTs. We supposed that the atelectasis may be related with irradiation to bronchus around lesions (Supplement Fig. 3).

3.3. Univariate and multivariate analyses and development of nomogram

Univariate analysis showed that per fraction dose ($p < 0.0001$, OR = 1.536, 95% CI = 1.221–1.933) were observed an obviously statistical significance with mass-like pattern, age ($p = 0.057$, OR = 1.048, 95% CI = 0.999–1.100) and prescription isodose line ($p = 0.076$, OR = 6.681, 95% CI = 0.315–14.2) showed a trend to associate with mass-like pattern. However, no correlation was found between other clinical or dosimetric factors (eg. sex, tumor location, tumor size, acute injury, PTV volume, V10 of total lung, V20 of total lung, Dmean of total lung and Dmax in PTV) and late injury patterns (Table 2). To avoid

important factors missing, we included parameters with $p < 0.1$ into multivariate analysis.

According to multivariate logistic regression analysis, we found that age ($p = 0.089$, OR = 1.049, 95% CI = 0.993–1.108), per fraction dose ($p < 0.0001$, OR = 1.573, 95% CI = 1.234–1.108) and prescription isodose line ($p = 0.027$, OR = 6.423, 95% CI = 5.944–6.956) were all included in the equation (Table 2). Hence, we included three parameters into the establishment of nomogram. The ROC curve of mass-like pattern predictive model showed that the AUC of nomogram model was 0.767 (95% CI = 0.677–0.857; sensitivity = 78%, specificity = 72.3%), which were better than each factor along (age: AUC = 0.604, 95% CI = 0.490–0.715; per fraction dose: AUC = 0.713, 95% CI = 0.609–0.817; prescription isodose line: AUC = 0.580, 95% CI = 0.470–0.691) (Fig. 4, Supplement Table 1).

4. Discussion

Previous studies have shown that local control of SBRT for early stage lung cancer was excellent [8–11], which leads to the extensive utilization of SBRT in clinical practice. At 2018 American Society of clinical Oncology (ASCO) annual meeting, Alexander Louie presented the long-term follow-up result of phase II study (JCOG 0403) of SBRT for 64 operable T1N0M0 NSCLC patients, this study shown that 3-year, 5-year, and 10-year OS were 76.5%, 54.0% and 23.8%, respectively [12]. Otherwise, RTOG 0618 have shown that 4-year local control rate of SBRT for operable early-stage lung cancer was 96% [13]. With the extensively practicing of SBRT in clinic, how to well characterized the radiographic changes after SBRT is becoming extraordinarily eager.

According to the radiobiological theory, the very high doses of per fraction may have a stronger effect for late injury than early injury. Our preliminary screen of CT images observed that only 36.8% patients occurred acute lung injury and 87.7% patients occurred late lung injury, which was consistent with the radiological theory. We describe radiological findings of lung cancer patients after SBRT in our institution. The majority of patients (85.8%) received three types of dose fractionation, 50 Gy/5Fx, 50 Gy/4Fx and 60 Gy/8Fx. The most common late injury pattern was mass-like pattern (39.6%), next was modified conventional pattern (33.0%). The results were different from various studies, Trovo et al. [14] observed a 44% modified conventional pattern at 13 to 18 months after SBRT, Faruqi et al. [15] seen an approximately 52% of this pattern after 12 months. The distributions of late injury pattern according to Koenig were different among different literatures [15–17]. This discrepancy may result from the following reasons. First, these studies were on different race which was the basic physical differences. Second, the per fraction dose was not uniform which influenced the late radiation injury seriously. Third, the description of Koenig's classification was ambiguous and researchers may have heterogeneity in understanding, especially for modified conventional pattern. An important and non-negligible problem is that these complicated injury patterns resulting in the misdiagnosis in clinical practice.

As we all know, accurate judgment of lung injury of tumor progression was both important to patients' emotion and treatment decision. We reviewed the chest CT reports from radiation oncologist and analyzed their diagnosis descriptions. Although most radiologists described the CT images objectively (62.3%), 24.5% RIL cases were still misdiagnosed with tumor progression. Most misdiagnosed lesions were mass-like pattern, which was indeed difficult to distinguish. We can only judge by long-term follow up and PET-CT. By radiological theoretical knowledge, visual judgment and experience still could not distinguish lung injury and tumor progression accurately. Thus, we need more information, especially objective parameters, to assist the radiologist' diagnosis. A previous study showed that imaging texture analysis may automatically predict lung cancer recurrence after SBRT [18], but the sensitivity and specificity were not satisfactory. Otherwise, researchers [19] also judge tumor response by PET-CT which was

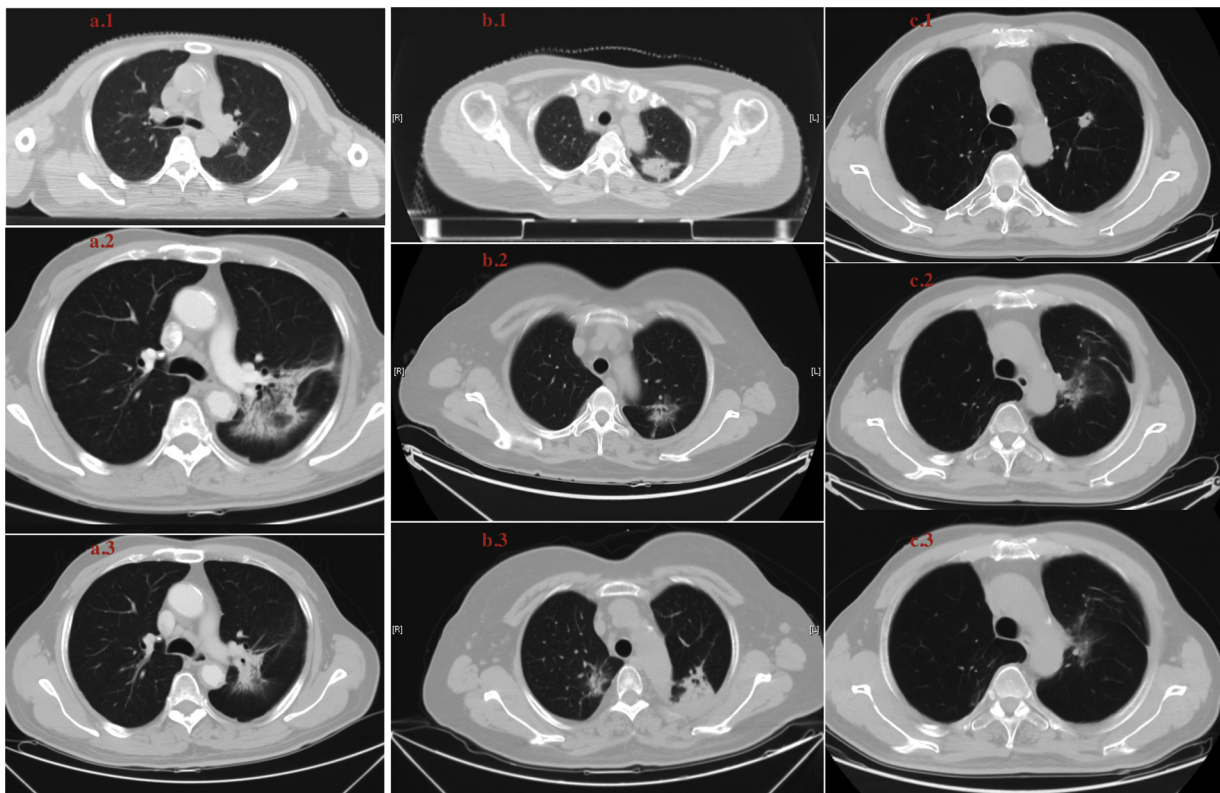


Fig. 1. Comparison of CT appearance before and after radiotherapy. a. Acute lung injury and modified conventional pattern. a.1. before SBRT, a.2. 4 months after SBRT, a.3. 1 year after SBRT. b. Non-acute lung injury and mass-like pattern. b.1. before SBRT, b.2. 2 months after SBRT, b.3. 9 months after SBRT. c. Acute lung injury and scar-like pattern. c.1. before SBRT, c.2. 5 months after SBRT, c.3. 18months after SBRT.

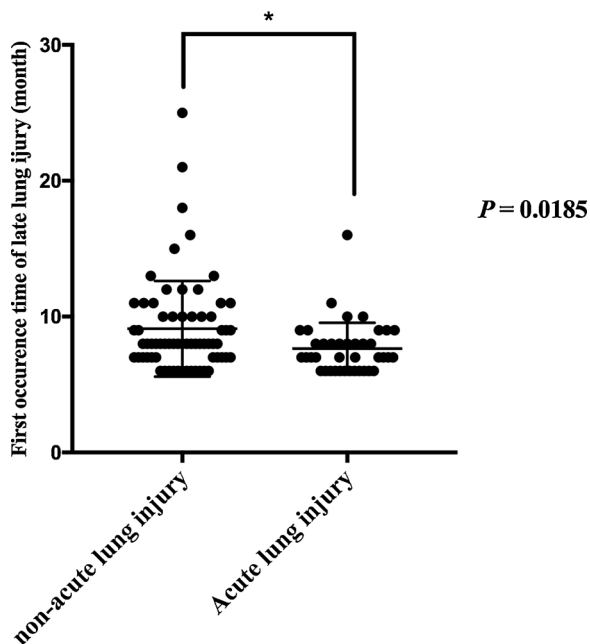


Fig. 2. Correlation between the first occurrence time of late injury and acute injury. Patients who showed acute injury trend to occur late lung injury earlier than patients who were not found acute injury.

relatively a better way to distinguish tumor progression and late radiation injury. Due to ionizing damage to health, PET-CT could not be frequently used in follow-up and it was a high economic cost for patients.

Hence, to assist radiologist' diagnosis, we developed a nomogram to

predict the occurrence of mass-like pattern injury. By univariate and multivariate analysis, we observed age, per fraction dose and prescription isodose line may related to the occurrence of mass-like pattern injury. A nomogram was established based on above three parameters and this predictive model showed a potential predictive value in clinic. Hence, in our knowledge, this predictive model may have a good help for clinical practice before a better assistant appearing. However, this is a relatively small sample size study, hence, when interpreting the value of the predictive nomogram, the statistical performance of the internal validation of ROC curve should be mentioned. And a large sample size and external validation study in multi-institution is needed.

Otherwise, with the rapid development of artificial intelligence (AI), we believe that AI may make a good job to distinguish tumor recurrence and radiotherapy damage, which would be more accurate and efficient combining theoretical knowledge, visual judgment and experience. Our research group studies showed that epithelial growth factor receptor (EGFR) mutations could be detected on CT images of patients with lung adenocarcinoma using radiomics and/or multi-level residual convolutionary neural networks [20]. With this basis, we also plan to conduct radiomics studies with AI on the diagnosis of lung injury pattern after SBRT.

By correlation analysis, we also found that no correlation between regular dosimetric factors (V_{10} of total lung, V_{20} of total lung and D_{mean} of total lung) and injury patterns. The main reason may be that V_{10} of total lung in 99.1% lesions were no more than 20 Gy and V_{20} of total lung in 100% lesion were no more than 10 Gy, which were strictly uniform to our institution SBRT treatment system [21]. In addition, to verify the safety of SBRT for lung cancer patients, we reclassified the late injury grade according to CTC 5.0. After reviewing the CT images of patients after SBRT and medical record, we observed that 87.7% patients were grade I lung fibrosis and the remaining patients were classified into grade 0. No grade 2–5 lung fibrosis was observed. A part of patients occurred atelectasis after SBRT. In this analysis, 13 (12.3%)

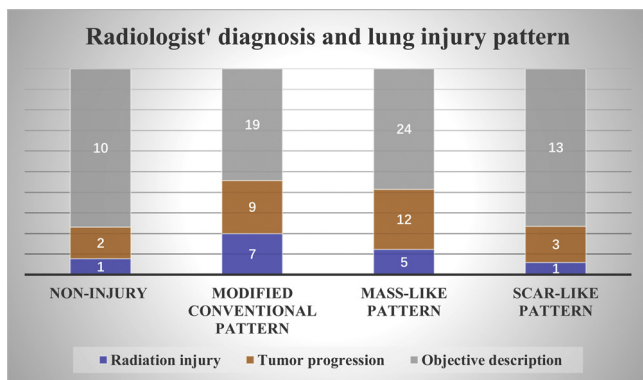


Fig. 3. The distribution of radiologist' diagnosis for radiotherapy lung injury pattern.

patients were observed with atelectasis. Manyan et al. represented validation of RTOG 0813 normal tissue constraints for pulmonary toxicity for SBRT in central NSCLC [22], which showed that the constraint of PBT affects the non-pneumonitis toxicity including atelectasis. They concluded that $D_{0.05} < 49.5$ Gy to the PBT have the highest sensitivity and specificity for toxicity prediction. An additional constraint of $D_{0.33} < 46.5$ Gy should be considered to avoid of Grade 3–5 non-

pneumonitis pulmonary toxicity. In our study, we also observed the similar phenomenon. We reviewed patients' radiotherapy plan, outlined the PBT and recomputed the irradiation dose. We found that some patients with atelectasis indeed received a high radiation dose to PBTs. Because the imaging quality of our CT scanner was poor, it's feasible to delineate PBT on part of total patients. Hence, a prospective study with high CT image quality should be conducted to confirm this suppose.

Several limitations exist in this study. First, this is a retrospective study, selective bias is inevitable. Second, this is a relatively small sample size study. Third, although the internal validation was done, the external validation may make this result more convinced. Hence, a large sample size, prospective and external validation study in multi-institution is necessary.

5. Conclusion

Radiation injury after SBRT and tumor progression were difficult to distinguish from each other. In our institution, the majority of late RIL was mass-like pattern which is the easiest to induce misdiagnosis of radiologists. Multivariate analysis showed that age, per fraction dose and prescription isodose line are the independent risk factors to predict mass-like pattern. A nomogram was built based on the three factors and its efficiency was validated by ROC curve. Certainly, this study needs a further verification, but our work still can help radiologist' diagnosis

Table 2
Logistic regression and ROC curve analysis of clinical factors in predicting failure mode.

	Mass-like pattern (n = 41)	Not mass-like pattern (n = 65)	Univariate analysis OR (95%CI)	P_1 value	Multivariate analysis OR (95%CI)	P_2 value
Age (y) (continuous variable)	m [#] 69(49-84)	m [#] 66(36-81)	1.048(0.999-1.100)	0.057	1.049(0.993-1.108)	0.089
Tumor size(mm)	m [#] 20(13-46)	m [#] 23(10-62)	0.967(0.923-1.013)	0.155	-	-
ITV volume(cm ³)	m [#] 7.42(1.35-51.1)	m [#] 8.86(0.99-76.1)	0.975(0.942-1.010)	0.164	-	-
PTV volume (cm ³)	m [#] 25.48(11.71-107.13)	m [#] 33.97(7.83-159.56)	0.988(0.972-1.004)	0.147	-	-
Prescription isodose line	m [#] 85% (78%-96%)	m [#] 85% (77%-90%)	6.681(0.315-14.2)	0.076	6.423(5.944-6.956)	0.027
V ₁₀ of total lung (%)	m [#] 10% (4%-21%)	m [#] 10% (3%-27%)	2.259(0.001-8040.05)	0.845	-	-
V ₂₀ of total lung (%)	m [#] 4% (2%-13%)	m [#] 5% (1%-18%)	0.049(0.000-25890.36)	0.654	-	-
Dmean of total lung	m [#] 3.5(1.44-7.89)	m [#] 3.77 (1.19-8.37)	0.970(0.742-1.267)	0.822	-	-
Dmax in PTV	m [#] 71.39(55.47-85.84)	m [#] 75.27(7.52-98.34)	0.987(0.956-1.018)	0.400	-	-
Sex				0.144	-	-
Female	17	18	1.850(0.810-4.222)			
Male	24	47				
Location			0.775(0.304-1.977)	0.594	-	-
Central	7	13				
Peripheral	34	52				
Dose of per fraction (Gy)			1.536(1.221-1.933)	< 0.0001	1.573(1.234-1.108)	< 0.0001
5	2	2				
6	1	8				
7	7	7				
7.5	2	24				
10	23	24				
12.5	11	4				
Total Dose (Gy)			0.991(0.935-1.049)	0.750	-	-
30	0	4				
50	36	41				
60	3	18				
70	2	2				
Acute injury			0.778(0.534-1.756)	0.545	-	-
No	27	39				
Yes	14	26				
Chemotherapy			0.960(0.431-2.137)	0.920	-	-
No	25	39				
Yes	16	26				

For continuous variables, "m" means median, () are ranges of variables.

All of three factors (age, per fraction dose and prescription isodose line) were in equation of multivariate analysis of logistic regression, hence, we included all of three parameters into nomogram.

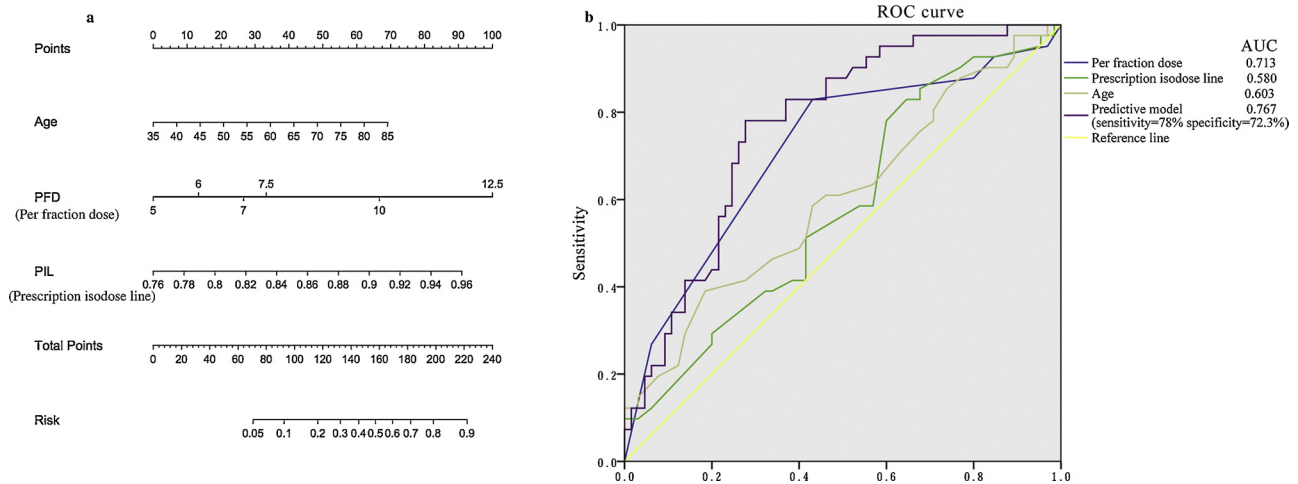


Fig. 4. The nomogram and ROC curve. (a) Nomogram predicting mass-like pattern. For each individual patient, three lines are drawn upward to determine the points received from the three variables in the nomogram. The sum of these points is located on the “Total Points” axis, and a line is drawn downward to determine the likelihood of this patient to occur distant failure. (b) The ROC curve of predictive factors and predictive model. The AUC of the model was 0.767, which was better than any factors along. The sensitivity and specificity of the predictive model were 78% and 72.3%, respectively.

and clinical practice.

Disclosure of potential conflict of interest

The authors declare that they have no conflict of interest.

Ethical approval

This article does not contain any studies with human participants performed by any of the authors.

Informed consent

For this type of study, formal consent is not required.

Declaration of Competing Interest

None.

Acknowledgements

This study was supported by the National Key Research and Development Program of China (2016YFC0905502) & Innovation Fund for PhD Students from Shanghai Jiao Tong University School of Medicine (CBXJ201814) & Project of multi-center clinical research, Shanghai Jiao Tong University School of Medicine (DLY201619) & Shanghai Chest Hospital Project of Collaborative Innovation (YJXT20190101).

Appendix A. Supplementary data

Supplementary material related to this article can be found, in the online version, at doi:<https://doi.org/10.1016/j.ejrad.2019.108708>.

References

- [1] National Comprehensive Cancer Network, NCCN Clinical Practice Guidelines in Oncology, Non-Small Cell Lung Cancer, Version 3, (2019) (Accessed 18 January 2019), https://www.nccn.org/professionals/physician_gls/pdf/nscl.pdf.
- [2] P. Murray, K. Franks, G.G. Hanna, A systematic review of outcomes following stereotactic ablative radiotherapy in the treatment of early-stage primary lung cancer, *Br. J. Radiol.* 90 (1071) (2017) 20160732.
- [3] H. Bahig, H. Chen, A.V. Louie, Surgery versus SABR for early stage non-small cell lung cancer: the moving target of equipoise, *J. Thorac. Dis.* 9 (4) (2017) 953–956.
- [4] L. HI, Thoracic radiotherapy change, Iatrogenic Thoracic Complications, (1983), pp. 141–160.
- [5] J.M. Brown, D.J. Carlson, D.J. Brenner, The tumor radiobiology of SRS and SBRT: are more than the 5 Rs involved? *Int. J. Radiat. Oncol. Biol. Phys.* 88 (2) (2014) 254–262.
- [6] T.R. Koenig, R.F. Munden, J.J. Erasmus, B.S. Sabloff, G.W. Gladish, R. Komaki, C.W. Stevens, Radiation injury of the lung after three-dimensional conformal radiation therapy, *AJR Am. J. Roentgenol.* 178 (6) (2002) 1383–1388.
- [7] SERVICES USDOHAH, NATIONAL CANCER INSTITUTE, Common Terminology Criteria for Adverse Events (CTCAE) Version 5.0, (2017) November 2017 https://ctep.cancer.gov/protocolDevelopment/electronic_applications/ctctm#ctc.50.
- [8] N. Shaverdian, D. Veruttipong, J. Wang, D. Schae, P. Kupelian, P. Lee, Pretreatment immune parameters predict for overall survival and toxicity in early-stage non-small-cell lung cancer patients treated with stereotactic body radiation therapy, *Clin. Lung Cancer* 17 (1) (2016) 39–46.
- [9] A. Navarro-Martin, S. Aso, J. Cacicedo, M. Arnaiz, V. Navarro, S. Rosales, R. de Blas, R. Ramos, F. Guedea, Phase II trial of SBRT for stage I NSCLC: survival, local control, and lung function at 36 months, *J. Thorac. Oncol.* 11 (7) (2016) 1101–1111.
- [10] J.Y. Chang, S. Senan, M.A. Paul, R.J. Mehran, A.V. Louie, P. Balter, H.J. Groen, S.E. McRae, J. Widder, L. Feng, et al., Stereotactic ablative radiotherapy versus lobectomy for operable stage I non-small-cell lung cancer: a pooled analysis of two randomised trials, *Lancet Oncol.* 16 (6) (2015) 630–637.
- [11] L. Murray, S. Ramasamy, J. Lilley, M. Snee, K. Clarke, H.B. Musunuru, A. Needham, R. Turner, V. Sangha, M. Flatley, et al., Stereotactic ablative radiotherapy (SABR) in patients with medically inoperable peripheral early stage lung cancer: outcomes for the first UK SABR cohort, *Clin. Oncol.* 28 (1) (2016) 4–12.
- [12] W.A. Stokes, M.R. Bronsert, R.A. Meguid, M.G. Blum, B.L. Jones, M. Koshy, D.J. Sher, A.V. Louie, D.A. Palma, S. Senan, et al., Post-treatment mortality after surgery and stereotactic body radiotherapy for early-stage non-small-cell lung cancer, *J. Clin. Oncol.* 36 (7) (2018) 642–651.
- [13] R.D. Timmerman, R. Paulus, H.I. Pass, E.M. Gore, M.J. Edelman, J. Galvin, W.L. Straube, L.A. Nedzi, R.C. McGarry, C.G. Robinson, et al., Stereotactic body radiation therapy for operable early-stage lung cancer: findings from the NRG oncology RTOG 0618 Trial Stereotactic body radiation therapy for operable early-stage lung Cancer Stereotactic body radiation therapy for operable early-stage lung cancer, *JAMA Oncol.* 4 (9) (2018) 1263–1266.
- [14] M.L.A. Trovo, I. El Naqa, C. Javidan-Nejad, J. Bradley, Early and late lung radiographic injury following stereotactic body radiation therapy (SBRT), *Lung Cancer (Amsterdam, Netherlands)* 69 (2010) 77–85.
- [15] S. Faruqi, M.E. Giuliani, H. Raziee, M.L. Yap, H. Roberts, L.W. Le, A. Brade, J. Cho, A. Sun, A. Bezjak, et al., Interrater reliability of the categorization of late radiographic changes after lung stereotactic body radiation therapy, *Int. J. Radiat. Oncol. Biol. Phys.* 89 (5) (2014) 1076–1083.
- [16] M. Dahele, D. Palma, F. Lagerwaard, B. Slotman, S. Senan, Radiological changes after stereotactic radiotherapy for stage I lung cancer, *J. Thorac. Oncol.* 6 (7) (2011) 1221–1228.
- [17] M. Trovo, A. Linda, I. El Naqa, C. Javidan-Nejad, J. Bradley, Early and late lung radiographic injury following stereotactic body radiation therapy (SBRT), *Lung Cancer (Amsterdam, Netherlands)* 69 (1) (2010) 77–85.
- [18] S.A. Mattonen, S. Tetar, D.A. Palma, A.V. Louie, S. Senan, A.D. Ward, Imaging texture analysis for automated prediction of lung cancer recurrence after stereotactic radiotherapy, *J. Med. Imaging (Bellingham, Wash)* 2 (4) (2015) 041010.
- [19] X. Zhang, H. Liu, P. Balter, P.K. Allen, R. Komaki, T. Pan, H.H. Chuang, J.Y. Chang, Positron emission tomography for assessing local failure after stereotactic body radiotherapy for non-small-cell lung cancer, *Int. J. Radiat. Oncol. Biol. Phys.* 83 (5) (2012) 1558–1565.

- [20] X.-Y. Li, J. Xiong, T.-Y. Jia, T.-L. Shen, R.-P. Hou, J. Zhao, X.-L. Fu, Detection of epithelial growth factor receptor (EGFR) mutations on CT images of patients with lung adenocarcinoma using radiomics and/or multi-level residual convolutionary neural networks, *J. Thorac. Dis.* 10 (2018).
- [21] B.D. Kavanagh, R. Timmerman, J.L. Meyer, The expanding roles of stereotactic body radiation therapy and oligofractionation: toward a new practice of radiotherapy, *Front. Radiat. Ther. Oncol.* 43 (2011) 370–381.
- [22] B. Manyam, K. Verdecchia, G.M. Videtic, T. Zhuang, N.M. Woody, K.L. Stephans, Validation of RTOG 0813 normal tissue constraints for pulmonary toxicity for stereotactic body radiation therapy in central non-small cell lung Cancer, *Int. J. Radiat. Oncol.* 102 (3, Supplement) (2018) S10.